Adsorption studies on metal alloy surfaces of Pt_3Sn with STM, LEIS and XPD.

S. Speller[1,2], M. Hoheisel[1], J. Kuntze[3], W. Heiland[1], A. Atrei[4], U. Bardi[5]

[1] Fachbereich Physik, Universität Osnabrück, D-49069 Osnabrück, Germany

[2] RIM, University of Nijmegen, NL-6525 ED Nijmegen, The Netherlands

[3] Institut für Exp. und Angew. Physik, Universität Kiel, D-24098 Kiel, Germany

[4] Dipartimento di Scienze e Techn. Chimiche, Universita di Siena, I-53100 Siena, Italy

[5] Dipartimento di Chimica, Universita di Firenze, I-50121 Firenze, Italy

Abstract

The three low-index surfaces of the metallic, ordered alloy Pt_3Sn have been studied by LEED (low energy electron diffraction), RHEED (reflection high energy electron diffraction, AES (Auger electron spectroscopy), STM (scanning tunneling microscopy), and LEIS (low energy ion scattering). During the usual preparation by sputtering and annealing of the surfaces depletion of Sn is observed due to preferential sputtering. Annealing restores the stoichiometric concentration eventually. At moderate annealing temperatures the different surfaces show characteristic structures. The (001) surfaces develops squared pyramids with {102} and {104}facets. The (111) surface shows a honeycomb structure caused by misfit dislocations. At that annealing stage a LEED $(\sqrt{3} \times \sqrt{3})$ R30°pattern is observed, confirmed by the STM topographic data. The (110) surface has steps and facets parallel to the [1-10] surface directions. The facets have the {102} orientation as the pyramid faces on (001). The fully annealed surfaces approach the bulk determination but are different in some details. The (001) is bulk terminated showing a c(2x2) LEED pattern. The large flat terraces are bordered by double steps and are decorated with single atomic rows of Pt. The fully annealed (111) surface is in a p(2x2) phase, whereas the (110) surface develops the bulk terminated structure, which is (2x1), with a favorization of the Sn rich possibility. The terraces are bordered by double steps. On the terraces single Sn vacancies are found. These surfaces provide interesting templates for the study of adsorption of CO and O.

Introduction

The Pt_3Sn alloy belongs into the chemically ordered Ll2 crystallographic class. The alloy is of interest for catalytic processing [1-3]. We have studied the three low index surfaces (001), (111) and (110) with STM mainly[4-6] because previous LEED, LEIS and x-ray diffraction studies had left some open question with respect to the chemical composition of the outermost

layer and with respect to the surface structure [7-12]. In general the surfaces show different states depending on the preparation. Clearly after the usual sputter cleaning there is a Sn depletion and disorder at the surface causing fuzzy LEED spots and Pt enhanced LEIS spectra. Furthermore there are two stages of annealing at moderate temperatures of approximately 600 K and at high temperatures of approximately 1000 K. On the (001) surface after 600 K annealing a 'streaky' c(2x2) LEED pattern was observed which changed into satisfactory, sharp c(2x2) patterns after the high temperature anneal. On (111) the low temperature annealing produces preferably a $(\sqrt{3} \times \sqrt{3})$ R30°pattern which converts into the p(2x2) pattern of the bulk terminated structure upon the high temperature annealing. For the (110) surface streaky (1x1), (1x2) or rhombic structures have been reported depending on the preparation. Here we summarize the results of our previous studies [4-6] and report new results of our adsorption studies of CO and O on the annealed Pt_3Sn surfaces.

Experiment

The STM, AES and RHEED experiments are performed in a Omicron STM 1 system. For target preparation a separate UHV chamber is used. The target analysis with LEED and AES is done in the same UHV chamber as the STM studies. We have a reverse LEED system and a grazing incidence electron gun (STAIB) producing RHEED patterns on the LEED screen. This RHEED gun is used in combination with a 180 electrostatic energy analyzer (PHI) for the AES analysis. For target transfer we use a transfer system and the usual wobble stick. The LEIS results are from the UHV scattering chamber at the Universita di Firenze. Clean gases are fed into the system via standard valves. In the STM surfaces can be exposed to gases in the preparation chamber or in situ during STM runs.

Results, clean surfaces

The $Pt_3Sn(111)$ surface is tin depleted after sputtering which is necessary for cleaning. This can be analyzed by Auger electron spectroscopy (AES) [4,7,8]. Annealing at 600 K does not restore the stoichiometry at the surface (AES) but the surface is well ordered and shows a $(\sqrt{3} \times \sqrt{3})$ R30°pattern [4,7-10]. The STM topography result is shown in Fig. 1 in an overview, large scale image and in a high resolution image in comparison with a hard sphere model [4]. The small scale image shows the $\sqrt{3}$ structure, but the large scale image shows a honeycomb network additionally. This network is caused by the tin deficit in the top layers of the crystal. The tin deficit is balanced by the crystal forming misfit dislocations. Since the lattice constants of Pt ($a_{Pt} = 0.392$ nm) and of Pt_3Sn ($a_{Pt_3Sn} = 0.400$ nm) are different the Sn depletion induces tensile stress which can be relieved by dislocations. The topmost layer of the surface is in turn Sn enriched, as shown by LEIS, which leads to compressive stress. This is the interpretation of according XPD data [7] where buckling of Sn atoms was observed. After annealing to 1000 K the honeycomb network disappears, the stoichiometry is restored and a LEED p(2 x 2) pattern is observed. This pattern is equivalent to the bulk truncated structure, i. e. in case of a monoatomic crystal this is the (1 x 1) structure, the labeling p(2 x 2) is conventional for binary

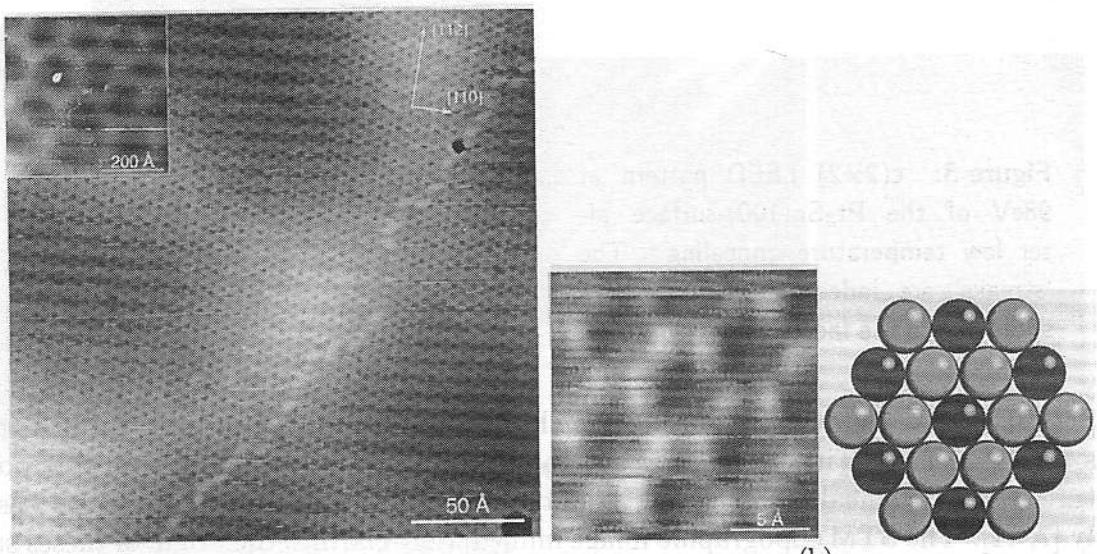

(a) (b)

Figure 1: STM-images of $Pt_3Sn(111)$ of the $(\sqrt{3}\times\sqrt{3})$ R30° structure taken after annealing to 600K, U_t=0.1V, I_t=0.5nA (a). The inset shows a $(530Å)^2$ terrace with the quasi-hexagonal hon eycomb-network. The main image is a close-up view of the inset's lower left region, size $(236Å)^2$. Both the atomic structure and the height modulation due to the honeycomb-network are visible. The irregular line running from the lower left to the upper right corner is a domain wall separating two different $(\sqrt{3}\times\sqrt{3})$ R30°-domains. It shows a defect in the upper right region. (b) $(17Å)^2$ high-resolution image (U_t=0.9V, I_t=1.0nA) and hard-sphere model of the $(\sqrt{3}\times\sqrt{3})$ R30° structure, as derived by crystallographic LEED [7]. Due to some drift the image is slightly elongated in the vertical direction. Pt corresponds to regions of high tunnel current (bright areas), Sn corresponds to regions of low tunnel current (dark areas).

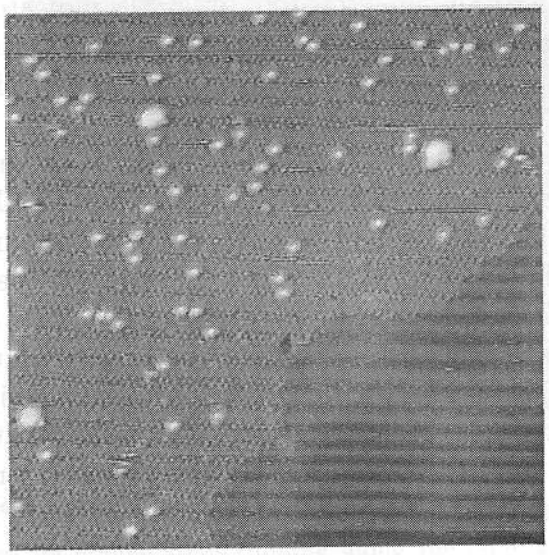

Figure 2: STM-image of $Pt_3Sn(111)$ of the mixed p(2×2) and $(\sqrt{3}\times\sqrt{3})$ R30° structure taken after annealing to 1000K, size $(44Å)^2$, U_t=0.9V, I_t=1.0nA. The image has been differentiated to enhance contrast. The small adatom islands mark the p(2×2) domain whereas in the lower right corner $(\sqrt{3}\times\sqrt{3})$ R30° areas with the honeycomb-network remain. The larger clusters may be due to residual contaminants, below the AES-detection-limit.

compounds. The STM topography agrees with the LEED findings, however, on the image white dots are visible (Fig. 2). These dots may be Sn adatom islands, remains of the surplus Sn in the top layer at lower annealing temperatures which is not incorporated into the bulk at the higher temperature.

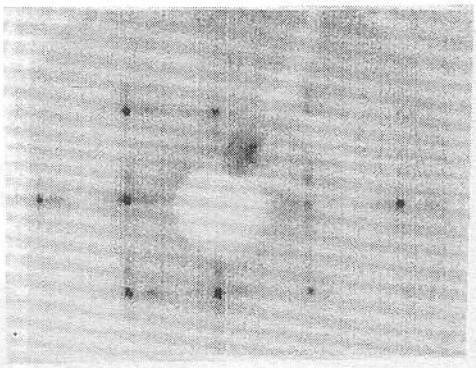

Figure 3: c(2×2) LEED pattern at 98eV of the $Pt_3Sn(100)$-surface after low temperature annealing. The 'streaks' are indeed ill defined facet spots due to the facets of the pyramids.

The $Pt_3Sn(001)$ surface shows with respect to the preferential sputtering of tin the same behavior as the (111) face. Tin is depleted, but the (001) face behaves quite different upon low temperature (600 K) annealing. The LEED pattern is streaky c(2 x 2) (Fig. 3) as observed previously [7, 11]. The STM topographic image immediately clarifies the origin of theses streaks (Fig.4) [5]. The streaks are facet beams caused by the faces of the pyramids seen in the STM image. The facets have (102) and (104) orientation mainly. The RHEED patterns of the pyramid decorated surface show typical transmission features. From the details of the RHEED data we conclude that the the pyramids are substitutionally disordered due to the tin depletion in the near surface region. As in case of the (111) face annealing at 1000 K restores the surface, the pyramids disappear and a c(2 x 2) LEED pattern with well defined spots is observed. The STM topographic image shows large flat terraces decorated with white, single atomic rows (Fig. 5). The steps bordering the terraces are all double steps. This finding is a strong argument for a termination with perfectly mixed Pt-Sn layers. Calculations of the electronic density of states suggest strongly that with the STM only Pt atoms are imaged. These calculations then suggest that the white rows are Pt atoms maybe of importance for catalytic activities.

The $Pt_3Sn(110)$ surface differs with respect to the preferential sputtering from the other two surfaces studied here. The AES data show the initial Sn depletion too, but LEIS indicates an initial Pt enrichment in top surface layer. After the low temperature annealing the situation is similar to the (111) face, i. e. the subsurface region is Sn depleted and the topmost layer is Sn enriched. After the 1000 K annealing ‚normality' is reached with (110) too (Fig. 6) [6]. The LEED pattern after the 600 K annealing contains (1 x 1), (1 x 2) and facet spots in agreement with previous studies [10,12]. The STM topographic image reveals the origin of the LEED spots (Fig. 7). The surface is faceted with {102} facets running parallel to the [001] surface directions. The facets have very likely not the bulk truncation composition (for further details see [6]). After annealing to 1000 K large, flat surfaces are formed with double steps (Fig. 8 a). Small area scans reveal dark spots, i. e. missing atoms (Fig. 8 b). The visible(‚white') atoms are very likely Pt forming the closed packed (1-10) rows. The Sn atoms are essentially invisble, when missing, are imaged as black spots. In other words, the annealed structure has Pt atoms in the topmost layer only, but, in point of view of the LEIS data (Fig. 6), the second layer is a complete Sn layer with a few vacancies. The different structures observed on the three Pt_3Sn faces studied here are summarized in Table I.

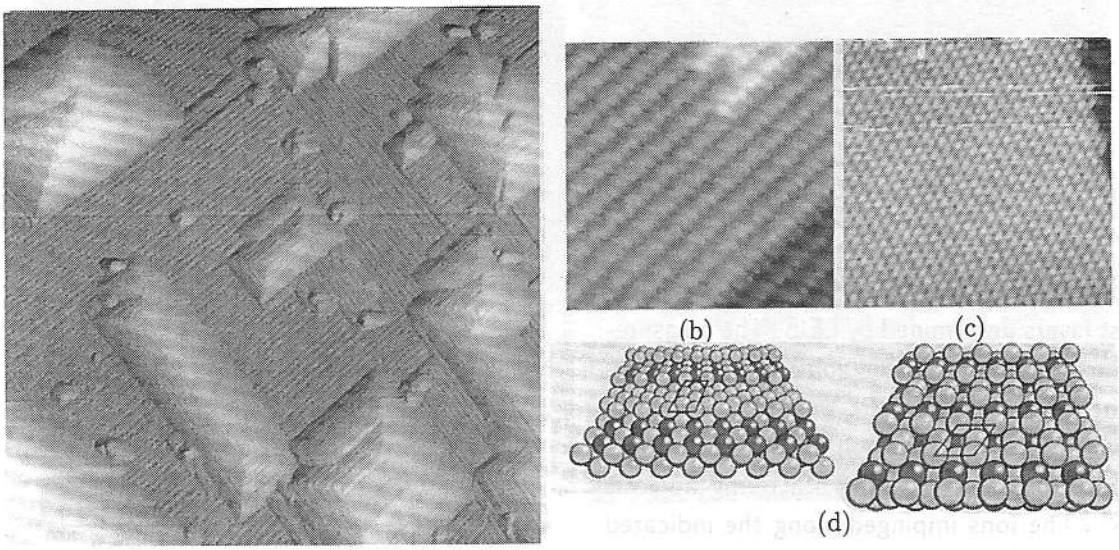

Figure 4: STM images (a-c) and marble models (d) of the $Pt_3Sn(001)$-surface after low temperature annealing. a)Overview, scan width $(1600Å)^2$, U_g=0.6V, I_t=1.0nA. b)(104)-facet on the side of a pyramid near the top. Scan width $(100Å)^2$, U_g=0.2V, I_t=1.0nA. c)(102)-facet on the side of a pyramid near the base. Scan width $(120Å)^2$, U_g=0.4V, I_t=1.0nA. d)Marble models of the (104)-facet (left panel) and the (102)-facet (right panel). For better visibility the models correspond to a chemically ordered bulk (Pt atoms light grey, Sn atoms dark grey), whereas the real pyramids are substitutionally disordered in the bulk. The unit cells seen by STM are indicated.

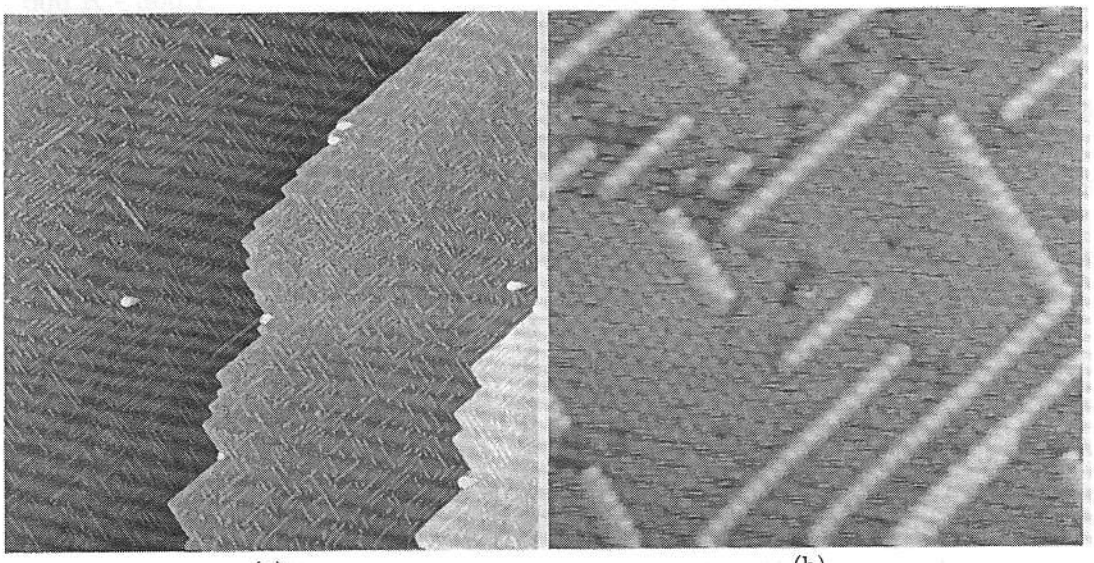

Figure 5: STM images of the $Pt_3Sn(001)$-surface after high temperature annealing (1000K). a)Overview, all steps are double steps running along the [100] and [010] directions. Scan width $(1700Å)^2$, U_g=0.9V, I_t=1.0nA. b) Close up view showing the remaining monoatomic rows and the substrate.The apparent height of the rows is 1Å. The square unit cell of the substrate shows no centered atoms, since only Pt is imaged (see text). Some defects are seen in the upper part of the image. Scan width $(160Å)^2$, U_g=10mV, I_t=1.0nA.

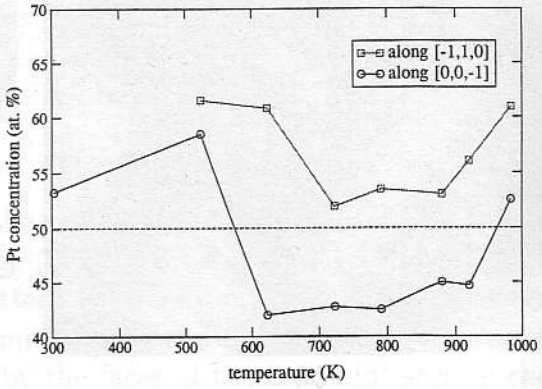

Figure 6: Pt concentration in the outermost layers determined by LEIS. The measurements were taken after sputtering and subsequent annealing of $Pt_3Sn(110)$. The He beam (1 keV) impinges on the sample surface with an angle of 45°, the scattering angle is 135°. The ions impinged along the indicated azimuthal directions.

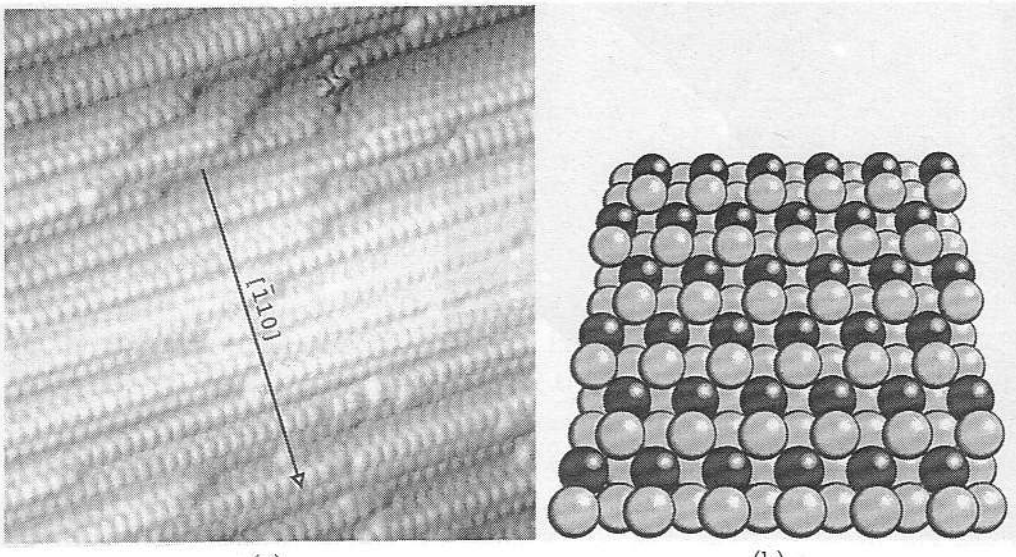

(a) (b)

Figure 7: STM image of the {102} facets on $Pt_3Sn(110)$ after anneal to 715 K, 154 Å, -0.15 V, 2.5 nA (a), and sphere model of a non-bulktruncated {102} facet (b), that is in accordance with the data.

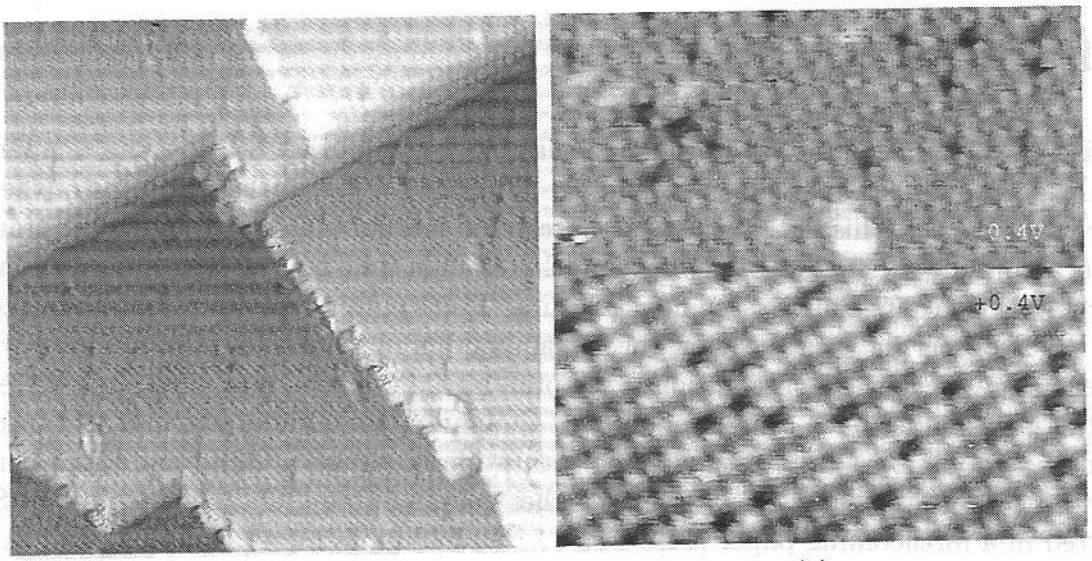

(a) (b)

Figure 8: STM images of the $Pt_3Sn(110)$ surface (a) merging double steps, 200 Å, 0.40 V, 0.8 nA. The $[00\bar{1}]$ steps form double, fourfold and sixfold steps whereas the $[\bar{1}10]$ steps are predominantly double. (b) 100 Å, +0.4 V (lower part) -0.4 V (upper part), 0.8 nA (b). The Pt atoms appear bigger when measuring the empty states (lower part). The contrast is higher when the filled states are measured (upper part). The big bump in the middle is presumably a contamination.

Table 1: Summary of the structures observed on Pt_3Sn surfaces after annealing at moderate and high temperature

	600 K - 800 K	1000 K -1100 K
(111)	$(\sqrt{3} \times \sqrt{3})$ R30°(Pt_2Sn), mesoscopic subsurface dislocation network	p(2×2) , adatom islands
(100)	multiple row structure, pyramids bordered by {102} and {104} facets	c(2×2) , double steps, single atomic ad rows
(110)	hill-and-valley-like structure with {102} facets	(2×1) , double steps, holes at Sn positions

Results, adsorption

We studied the adsorption of CO on well annealed $Pt_3Sn(110)$ (Fig. 8a) at room temperature. After an exposure of 60 Langmuirs CO is found adsorbed on top of the Pt atoms of the [1-10] surface rows (Fig. 9). This is the ‚classical' adsorption site for CO on Pt and other transition metals in accordance with the Blyholder model [13]. We find no CO adsorption at the step microfacets and no change of the step net structure. This suggests that the Step microfacets are Sn rich. When observing with the STM the CO adsorption in situ we find a high mobility of the CO molecules. Another new observation is the preferential assembling of the CO in dimers and tetramers. This implies both a high mobility of CO and a lateral interaction of CO seemingly saturating at about four. Interestingly, the saturation coverage is quite low (approximately 0.2 ML with respect to the Pt sublattice). Further details of the CO adsorption on Pt_3Sn will be reported in a forthcoming paper [14].

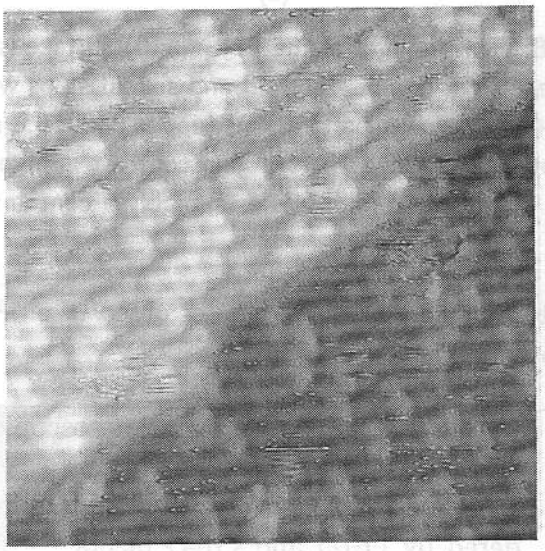

Figure 9: $Pt_3Sn(110)$ after exposure to 60 Langmuirs CO; 120 Å, 0.4 V, 0.8 nA. The CO is found on top of the Pt bumps and never inbetween at the Sn positions. The Carbon side binds to the Pt substrate atoms and the molecules are arranged in dimers and tetramers.

The adsorption of oxygen on the well annealed (1000 K) $Pt_3Sn(111)$ is a rather violent process in comparison to the CO adsorption [15]. Fig. 10 shows LEIS data after exposing the (111) surface to 4200 Langmuir O_2. The oxygen adsorption causes the LEIS Pt signal to disappear whereas the Sn signal is hardly affected. The LEIS ‚visibility' of the oxygen suggests that O is adsorbed on or at the surface. XPS analysis gives clear evidence that the O is bound to Sn whereas the Pt lines are not affected by the O adsorption. These data together with the LEIS evidence suggest the formation of a 2D tin oxide surface layer. This layer formation implies the segregation of Sn to the surface induced by the O adsorption. The LEED pattern of the O-exposed (111) surface shows a p(4 x 4) superstructure. In order to obtain good quality LEED patterns the surface is annealed at 740 K. The STM topographic images, after annealing at 740 K too, clarify the structure (Fig. 11 a and b). The order extends over large areas. The white ‚bumps' can not be identified easily, as usual in STM topographic images. The white bumps, however, are ordered in the p(4 x 4) pattern as shown in Fig. 11 b. In a study of the oxidation of a $Pt_3Sn(111)$ surface alloy film is suggested that these bumps are Sn_xO_y agglomerates [16]. A variation of the gap voltage does not change the appearance of the bumps indicating metallic properties of the tin oxide surface layer. The structure contains some defects as can be seen in Fig 11 b. It is interesting to note that upon oxygen adsorption the step structure is affected

too. Further aspects of the structure of the tin oxide layers are found using XPD which will be published separately [15].

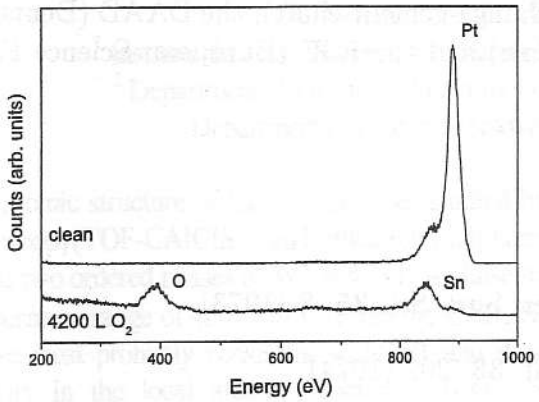

Figure 10: LEIS spectra (1000 eV He^+) from the clean surface (top) and after exposing it to 4200 L O_2 (bottom). The incidence angle was 45° and the scattering angle 135°. The Pt present before the oxidation disappears, O emerges.

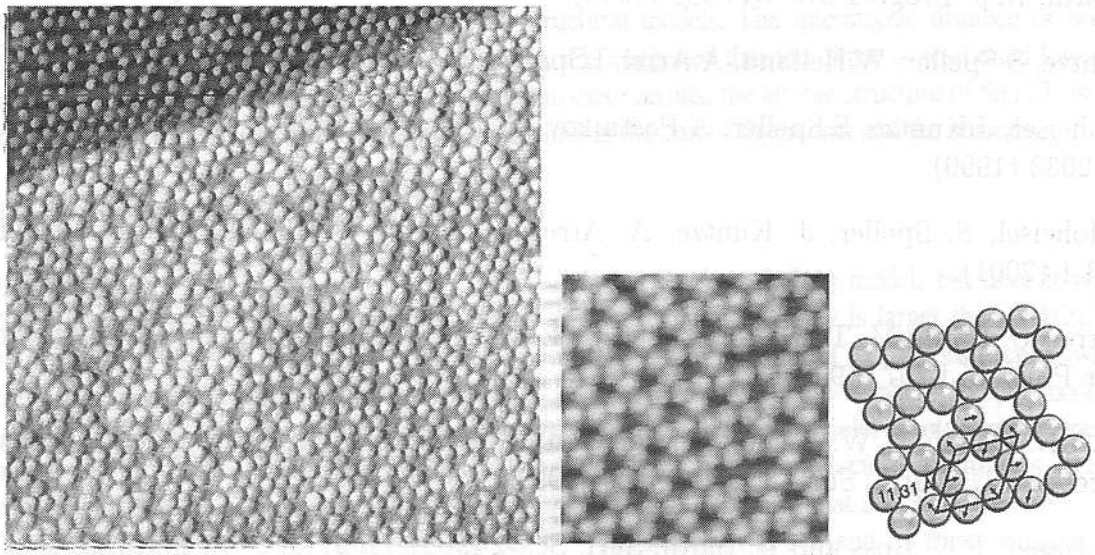

Figure 11: (a) STM image of $Pt_3Sn(111)$ (200 Å^2, $U_T = +0.5$ V, $I_T = 0.8$ A) after exposure to 3000 L O_2 at 740 K. The surface structure is governed by the p(4×4) structure. (b) The $Pt_3Sn(111)$ p(4×4) structure: small-scale STM image (68 Å^2, $U_T = +0.5$ V, $I_T = 0.8$ A), sphere model (The balls represent one bump from the STM images each, in fact they might consist of more than one atom). A p(4×4) unit cell is shown, the displacement directions of the bumps as observed by STM are indicated. To improve clearness a larger displacement than measured is shown.

In summary we conclude that the Pt_3Sn system provides a rich variety of structures whether clean or upon adsorption of simple gases. There are the structures due to the tin depleted system and those of the well annealed surfaces (Table I). Upon adsorption structural changes are induced, especially oxygen causes a massive mass transport in the surface region.

Acknowledgments

This work is supported by the DFG (Deutsche Forschungs-gemeinschaft), the DAAD (Deutscher Akademischer Austauschdienst, VIGONI-Programme) and the ESF (European Science Foundation, ALEnet).

References

[1] R. Bowman, L. H. Toneman and A. A. Holscher, Surf. Sci. **35**, 8 (1973)

[2] R.A. van Santen and W.M.H. Sachtler, J. Catal. **33**, 202 (1974)

[3] U. Bardi, Rep. Progr. Phys. **57**, 939 (1994)

[4] J.Kuntze, S.Speller, W.Heiland, A.Atrei, I.Spolveri, U.Bardi, Phys.Rev.B **58** R16005 (1998)

[5] M.Hoheisel, J.Kuntze, S.Speller, A.Postnikov, W.Heiland, I.Spolveri, U. Bardi, Phys. Rev. B **60**, 2033 (1999).

[6] M. Hoheisel, S. Speller, J. Kuntze, A. Atrei, U. Bardi, W. Heiland, Phys. Rev. **B 63**, 245403-1 (2001).

[7] A. Atrei, U. Bardi, M. Torrini, E. Zanazzi, G. Rovida, H. Kasamura and M. Kudo, Condes. Matter Phys. **5**, L207 (1993)

[8] W.C.A.N. Celsen, A.W. Denier van der Gon, M.A. Reijme, H.H. Brongersma, I. Spolveri, A. Atrei and U. Bardi, Surf. Sci. **406**, 264 (1998)

[9] A.N. Haner, P.N. Ross and U. Bardi, Surf. Sci. **249**, 15 (1991)

[10] A. N. Haner, P. N. Ross and U. Bardi, Catal. Lett. **8**, 1 (1991)

[11] A. Atrei, U. Bardi, G. Rovida, M. Torrini, and E. Zanazzi, Phys. Rev. B **46**, 1649 (1992)

[12] A.N. Haner, P.N. Ross, U. Bardi, in *The Structure of Surfaces III*, Eds S.Y. Tong, M.A. Van Hove, K. Takayanagi, X.D. Xie, Springer, 1991

[13] G. Blyholder, J. Vac. Sci. Technol. **11**, 865 (1974).

[14] M. Hoheisel et al. to be published

[15] M. Hoheisel, S. Speller, W. Heiland, A. Atrei, U. Bardi and G. Rovida, Phys. Rev. B, submitted.

[16] M. Batzill, D.E. Beck, B.E, Koel, Appl. Phys. Lett. bf 78, 2766 (2001).